

Applications of Physiologically Based Pharmacokinetic Modeling of Rivaroxaban—Renal and Hepatic Impairment and Drug-Drug Interaction Potential

The Journal of Clinical Pharmacology
2021, 61(5) 656–665
© 2020 The Authors. *The Journal of Clinical Pharmacology* published by Wiley Periodicals LLC on behalf of American College of Clinical Pharmacology
DOI: 10.1002/jcph.1784

Stefan Willmann, PhD¹, Katrin Coboeken, PhD¹, Stefanie Kapsa, PhD², Kirstin Thelen, PhD², Markus Mundhenke, MD³, Kerstin Fischer, PhD⁴, Burkhard Hügl, MD⁵, and Wolfgang Mück, PhD²

Abstract

The non-vitamin K antagonist oral anticoagulant rivaroxaban is used in several thromboembolic disorders. Rivaroxaban is eliminated via both metabolic degradation and renal elimination as unchanged drug. Therefore, renal and hepatic impairment may reduce rivaroxaban clearance, and medications inhibiting these clearance pathways could lead to drug-drug interactions. This physiologically based pharmacokinetic (PBPK) study investigated the pharmacokinetic behavior of rivaroxaban in clinical situations where drug clearance is impaired. A PBPK model was developed using mass balance and bioavailability data from adults and qualified using clinically observed data. Renal and hepatic impairment were simulated by adjusting disease-specific parameters, and concomitant drug use was simulated by varying enzyme activity in virtual populations ($n = 1000$) and compared with pharmacokinetic predictions in virtual healthy populations and clinical observations. Rivaroxaban doses of 10 mg or 20 mg were used. Mild to moderate renal impairment had a minor effect on area under the concentration-time curve and maximum plasma concentration of rivaroxaban, whereas severe renal impairment caused a more pronounced increase in these parameters vs normal renal function. Area under the concentration-time curve and maximum plasma concentration increased with severity of hepatic impairment. These effects were smaller in the simulations compared with clinical observations. AUC and C_{\max} increased with the strength of cytochrome P450 3A4 and P-glycoprotein inhibitors in simulations and clinical observations. This PBPK model can be useful for estimating the effects of impaired drug clearance on rivaroxaban pharmacokinetics. Identifying other factors that affect the pharmacokinetics of rivaroxaban could facilitate the development of models that approximate real-world pharmacokinetics more accurately.

Keywords

drug-drug interaction, hepatic impairment, pharmacokinetics, physiologically based pharmacokinetic modeling, renal impairment, rivaroxaban

Rivaroxaban is an oral anticoagulant that directly inhibits factor Xa and has been approved for the prevention and treatment of several thromboembolic disorders in adult patients.^{1,2} The outcomes of several phase 3 studies have led to the approval of rivaroxaban for the prevention of venous thromboembolism after knee or hip replacement surgery and for the treatment and prevention of the recurrence of deep vein thrombosis and/or pulmonary embolism. In eligible patients with nonvalvular atrial fibrillation (AF), rivaroxaban is indicated to prevent stroke or systemic embolism. Additionally, in Europe, rivaroxaban 2.5 mg twice daily plus aspirin is approved for the prevention of atherothrombotic events after acute coronary syndrome and has recently been approved for the prevention of thromboembolic events in patients with coronary artery disease, peripheral artery disease, or both in several countries.^{1–3} Recently, rivaroxaban was investigated for thrombosis treatment in children^{4,5} and in patients with symptomatic peripheral artery disease undergoing lower-extremity revascularization.^{6,7}

Both the kidneys and the liver play an important role in rivaroxaban elimination. In addition, the liver synthesizes many factors of the coagulation pathway, and clotting factors are reduced in hepatically

¹Clinical Pharmacometrics, Bayer AG, Wuppertal, Germany

²Clinical Pharmacokinetics Cardiovascular, Bayer AG, Wuppertal, Germany

³Medical Affairs Cardiovascular, Bayer Vital GmbH, Leverkusen, Germany

⁴Bayer Healthcare, Köln, Germany

⁵Clinic for Cardiology and Rhythmology, Marienhaus Klinikum St Elisabeth Neuwied, Neuwied, Germany

This is an open access article under the terms of the Creative Commons Attribution-NonCommercial License, which permits use, distribution and reproduction in any medium, provided the original work is properly cited and is not used for commercial purposes.

Submitted for publication 27 February 2020; accepted 9 November 2020.

Corresponding Author:

Stefan Willmann, PhD, Clinical Pharmacometrics, Bayer AG, 42096 Wuppertal, Germany
Email: stefan.willmann@bayer.com

impaired patients.⁸ Rivaroxaban has a high bioavailability (>80%) for doses up to 10 mg. For the higher doses of rivaroxaban (15 mg and 20 mg), a similarly high bioavailability can be achieved when administered with food.² Rivaroxaban is highly bound to plasma proteins, mainly to serum albumin. Approximately two-thirds of a dose are subject to metabolic degradation by the cytochrome P450 (CYP) enzymes CYP3A4 and CYP2J2, as well as CYP-independent mechanisms, with approximately equal proportions of the metabolites being excreted renally and in the feces.^{9,10} Approximately one-third ($\approx 36\%$) of the dose is renally eliminated as unchanged drug, of which $\approx 7\%$ is excreted via glomerular filtration and $\approx 29\%$ via active renal secretion.^{9,11} In vitro and in vivo drug interaction studies suggest that transporters involved in active renal secretion of rivaroxaban include P-glycoprotein (P-gp) and breast cancer resistance protein (ABCG2).^{9,12,13}

If rivaroxaban is administered to patients with moderate renal impairment (creatinine clearance, 30-49 mL/min), dose adjustment may be required and renal function needs to be monitored appropriately, depending on the indication.^{2,14} The use of rivaroxaban in patients with a creatinine clearance of 15 to 29 mL/min has not been studied extensively, but the available evidence suggests that plasma concentrations of rivaroxaban are significantly increased and that the drug should therefore be used with caution in this patient population.² Moderate hepatic impairment (Child-Pugh B) leads to an increased area under the concentration-time curve (AUC) and increased factor Xa inhibition¹⁵; therefore, rivaroxaban should not be administered to patients with moderate (Child-Pugh B) and severe (Child-Pugh C) hepatic impairment or with any hepatic disease associated with coagulopathy. Furthermore, medications that are eliminated or metabolized by the same pathways as rivaroxaban have the potential to lead to drug-drug interactions (DDIs). Previous DDI studies have been conducted in healthy subjects, and the results suggest that only strong inhibitors of both CYP3A4 and P-gp interact with rivaroxaban at a clinically relevant level.¹⁶

A previous physiologically based pharmacokinetic (PBPK) modeling study explored the potential increase in rivaroxaban exposure in patients with renal or hepatic impairment and simultaneous administration of other drugs that inhibit CYP3A4 or P-gp.¹⁷ More recently, a weak DDI was predicted to exist between rivaroxaban and the antiarrhythmic drugs amiodarone and dronedarone.¹⁸ These antiarrhythmic drugs can be used as part of AF management and may therefore be administered concomitantly with rivaroxaban.^{19,20} Amiodarone is a second-choice antiarrhythmic agent for long-term rhythm control therapy that can be used in patients with abnormal left ventricular

hypertrophy or heart failure, whereas dronedarone can be used for long-term rhythm control in certain patients with no history of heart failure or left ventricular systolic dysfunction and with or without structural heart disease.²⁰⁻²² However, both amiodarone and dronedarone act as CYP3A4 and P-gp inhibitors. Dronedarone is primarily metabolized by CYP3A4 in the liver and is a mild inhibitor of CYP2D6, a moderate inhibitor of CYP3A4, and a potent inhibitor of P-gp.²² Amiodarone is also primarily metabolized by, and a weak inhibitor of, CYP3A4 and has the potential to inhibit other enzymes including CYP2D6 and P-gp.²¹ Based on the current evidence, both agents have the potential for DDIs with rivaroxaban in patients with AF.

The aim of this study was to apply a previously developed and validated PBPK model for rivaroxaban to simulate and extrapolate the pharmacokinetics (PK) of rivaroxaban to situations that have not yet been clinically tested, specifically to situations in which drug clearance may be impaired due to renal or hepatic impairment and concomitant use of drugs that inhibit rivaroxaban clearance pathways to different degrees.

Methods

The Rivaroxaban PBPK Model

An adult PBPK model was developed during the early development phase of rivaroxaban. This model was built using physicochemical data of rivaroxaban, mass balance information (Figure 1), as well as PK data obtained in healthy adult subjects. At first, a model was established to describe rivaroxaban PK following intravenous administration. This model was then expanded to account for oral administration under fasted and fed conditions.²³ The adult PBPK model was then qualified by comparing population simulations in a virtual reference population for 10-mg and 20-mg oral doses of rivaroxaban with corresponding clinically observed individual PK data observed in healthy adults that were not used for model building.^{23,24} The adult model was further scaled to children to support the pediatric development program of rivaroxaban. Details of the PBPK model building and qualification in adults and children have been published previously.²³

Software

The rivaroxaban PBPK model was built with the software PK-Sim Version 4.2 and exported to MoBi Version 2.3 (both from Bayer AG, Leverkusen, Germany, now available as part of the Open Systems Pharmacology Suite; www.open-systems-pharmacology.org). The underlying model of PK-Sim considers organ-specific blood flow rates and permeation across the cellular membrane into each organ that is driven by the substance- and organ-specific permeability \times surface

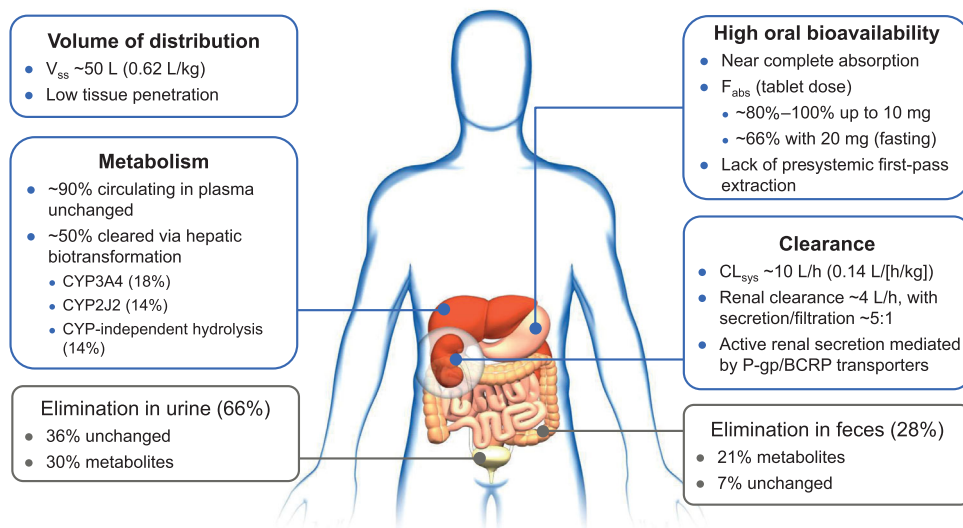


Figure 1. Rivaroxaban metabolic clearance and elimination pathways, based on in vitro investigations and human mass balance, absolute bioavailability, and renal impairment studies.^{14,23,24} Adapted from Mueck et al.¹⁴ BCRP, breast cancer resistance protein; CL_{sys} , systemic plasma clearance; CYP, cytochrome P450; F_{abs} , absolute oral bioavailability; P-gp, P-glycoprotein; V_{ss} , volume of distribution at steady state.

Table 1. Fractional Changes (Dimensionless) in PBPK Parameters That Are Altered in Renally Impaired Individuals vs Healthy Individuals

PBPK Model Parameter	Value
Portal vein blood flow ⁵⁵ (severe renal impairment)	1.267
Hepatic arterial blood flow ⁵⁵ (severe renal impairment)	0.373
Renal blood flow ⁵⁶ (severe renal impairment)	0.135
CYP3A activity ⁵⁷ (severe renal impairment)	0.860
CYP2J2 activity ^a	1.00
P-gp activity (mild renal impairment)	0.75
P-gp activity (moderate renal impairment)	0.50
P-gp activity (severe renal impairment)	0.25

CYP, cytochrome P450; PBPK, physiologically based pharmacokinetic; P-gp, P-glycoprotein.

^aUnchanged (no data available).

area product.²⁵ All batch-mode simulations for MoBi models were performed using MATLAB Version 8.2.0.701 (R2013b) and the MoBi Toolbox Version 2.3 for MATLAB (The MathWorks Inc., Natick, Massachusetts). The same MATLAB version was used for plotting.

Virtual Individuals and Populations

Renal and hepatic impairment were simulated in virtual populations. For each population, 1000 virtual individuals were created with the population simulation module of PK-Sim, and the population was converted to PK-Sim 4.2 format. For simulations in populations with renal or hepatic impairment, model parameters were adapted based on prior pathophysiologic knowledge as shown in Table 1 and Table 2, respectively. For CYP2J2, no specific disease-related activity data were available, and it was therefore assumed that its specific activity remained unchanged in the renal or hepatic

Table 2. Fractional Changes (Dimensionless) in PBPK Parameters That Are Altered in Hepatically Impaired Individuals vs Healthy Individuals²⁹

PBPK Model Parameter	Severity of Liver Disease		
	Child–Pugh A	Child–Pugh B	Child–Pugh C
Portal vein blood flow ⁵⁸	0.4	0.36	0.04
Hepatic arterial blood flow ⁵⁸	1.3	2.3	3.4
Renal blood flow ⁵⁹	0.88	0.65	0.48
Blood flow in other organs ⁵⁹	1.75	2.25	2.75
Albumin ^{60–62}	0.81	0.68	0.5
Alpha-I-acid glycoprotein ⁶³	0.6	0.56	0.3
Hematocrit (absolute) ⁶⁴	0.39	0.37	0.35
Hematocrit (fractional) ⁶⁴	0.91	0.86	0.81
Functional liver mass ⁶⁵	0.69	0.55	0.28
CYP3A4 activity ⁶⁶	1	0.4	0.4
CYP2J2 activity ^a	1	1	1
GFR ^{62,67,68}	1	0.7	0.36

CYP, cytochrome P450; GFR, glomerular filtration rate; PBPK, physiologically based pharmacokinetic.

^aUnchanged (no data available).

impairment model. However, the fractional plasma clearance via CYP2J2 (as well as for CYP3A4) is affected by the pathophysiologic changes in liver blood flow rate and the reduction in functional liver mass as listed in Table 1 and Table 2. Each “virtual” individual in the healthy and diseased populations has the same anthropometric and physiologic parameters and differs only in the specific disease parameters. For simulations of rivaroxaban PK in the presence of concomitant drugs, “virtual” individuals were generated with the same anthropometric and physiologic parameters and varying CYP3A4 and P-gp activity.

Parameter Sensitivity Analysis

The rivaroxaban PBPK model is parameterized based on prior knowledge using data and information from various sources. For example, the relative contributions of the different clearance pathways were informed by in vitro data⁹ as well as human mass balance data.¹⁰ Before using a PBPK model for predictions, it is important to understand how uncertainties in the model parameters influence the simulation results of the model. To this end, a parameter sensitivity analysis of the rivaroxaban PBPK model was performed. Parameter sensitivities were calculated by varying each model parameter separately by factors of 1.10, 1.05, 1/1.05, and 1/1.10 and calculating the slope of a linear regression line through the relative PK parameter change (here, AUC and maximum plasma concentration [C_{\max}]) vs the parameter variation. A list of the model parameters rank-ordered by their sensitivity provides an understanding of the most influential model parameters.

Categorization of Renal Impairment

Renal impairment categories were defined as follows (according to guidelines at the time of clinical studies): healthy (glomerular filtration rate [GFR], ≥ 80 mL/min), mild renal impairment (GFR, 50 to < 80 mL/min), moderate renal impairment (GFR, 30 to < 50 mL/min), and severe renal impairment (GFR, 0 to < 30 mL/min). In patients with chronic renal impairment, it was assumed that the increasing reduction in GFR was associated with a corresponding decrease in P-gp activity in the kidney (Table 1).

Categorization of CYP3A4 Enzyme Inhibition Levels

CYP3A4 inhibition categories were defined on the basis of the US Food and Drug Administration criteria,²⁶ using midazolam as the sensitive index substrate. Index inhibitors, such as ketoconazole, show predictable inhibition of a metabolic pathway or enzyme. A PBPK model for midazolam was used to calculate the AUC increase dependent on CYP3A4 activity level in the presence of ketoconazole. Static activity levels implemented as factorial changes (CYP3A4 factor) were identified that correspond to the threshold values for factorial AUC increase (Table 3).

Definition of P-glycoprotein Inhibition Categories

P-gp inhibition was arbitrarily classified into 4 categories: no inhibition (0% to $< 25\%$), weak inhibition (25% to $< 50\%$), weak to moderate inhibition (50% to $< 75\%$), and strong inhibition (75% to $< 100\%$).

Application of the Rivaroxaban PBPK Model

Simulations of the PK of rivaroxaban were conducted in virtual healthy and clearance-impaired populations. The PK parameters AUC and C_{\max} were analyzed in comparison with healthy populations. The PK of

Table 3. Classification of CYP3A4 Activity Based on the Relative AUC Increase for Midazolam

Classification of CYP3A4 Activity	AUC Increase	Level of CYP3A4 Activity at Upper Limit
No inhibition	< 1.25	84%
Weak inhibition	1.25 to < 2	58%
Moderate inhibition	2 to < 5	26%
Strong inhibition	≥ 5	$< 26\%$

AUC, area under the concentration-time curve; CYP, cytochrome P450.

rivaroxaban was also simulated in different DDI scenarios that were designed to approximately reflect the CYP3A4 enzyme and P-gp inhibition previously reported in clinical DDI studies.

Results

Sensitivity Analysis

For AUC, the parameter sensitivity analysis for a total of 237 PBPK model parameters revealed that the 23 most influential parameters contributed to 90% of the total sensitivity. The most influential model parameters for AUC can be grouped into 2 main categories:

1. *Physiologic parameters relevant for the oral absorption of rivaroxaban.* The dimensions of the gastrointestinal tract (segmental lengths, radiuses, and effective surface areas), as well as the gastric emptying time influence the AUC by modulating the extent of the oral absorption of rivaroxaban.
2. *Parameters relevant for the elimination of rivaroxaban.* The volumes of the liver and kidney and the fractional contributions of cells, vascular and interstitial space to their total volume, as well as kidney blood flow are the model parameters with highest sensitivity that influence AUC by modulating the rate and extent of rivaroxaban elimination.

For C_{\max} , the parameter sensitivity analysis revealed that 37 parameters contributed to 90% of the total sensitivity. The most influential model parameters for C_{\max} can be grouped into 3 main categories:

1. Physiologic parameters relevant for the oral absorption of rivaroxaban (as for AUC).
2. Parameters relevant for rivaroxaban elimination (as for AUC).
3. Physiologic parameters relevant for the distribution of rivaroxaban: volume and composition, as well as blood flow rate of the major distribution organs (muscle, fat tissue) affect the rate and extent of distribution of rivaroxaban between plasma and tissue.

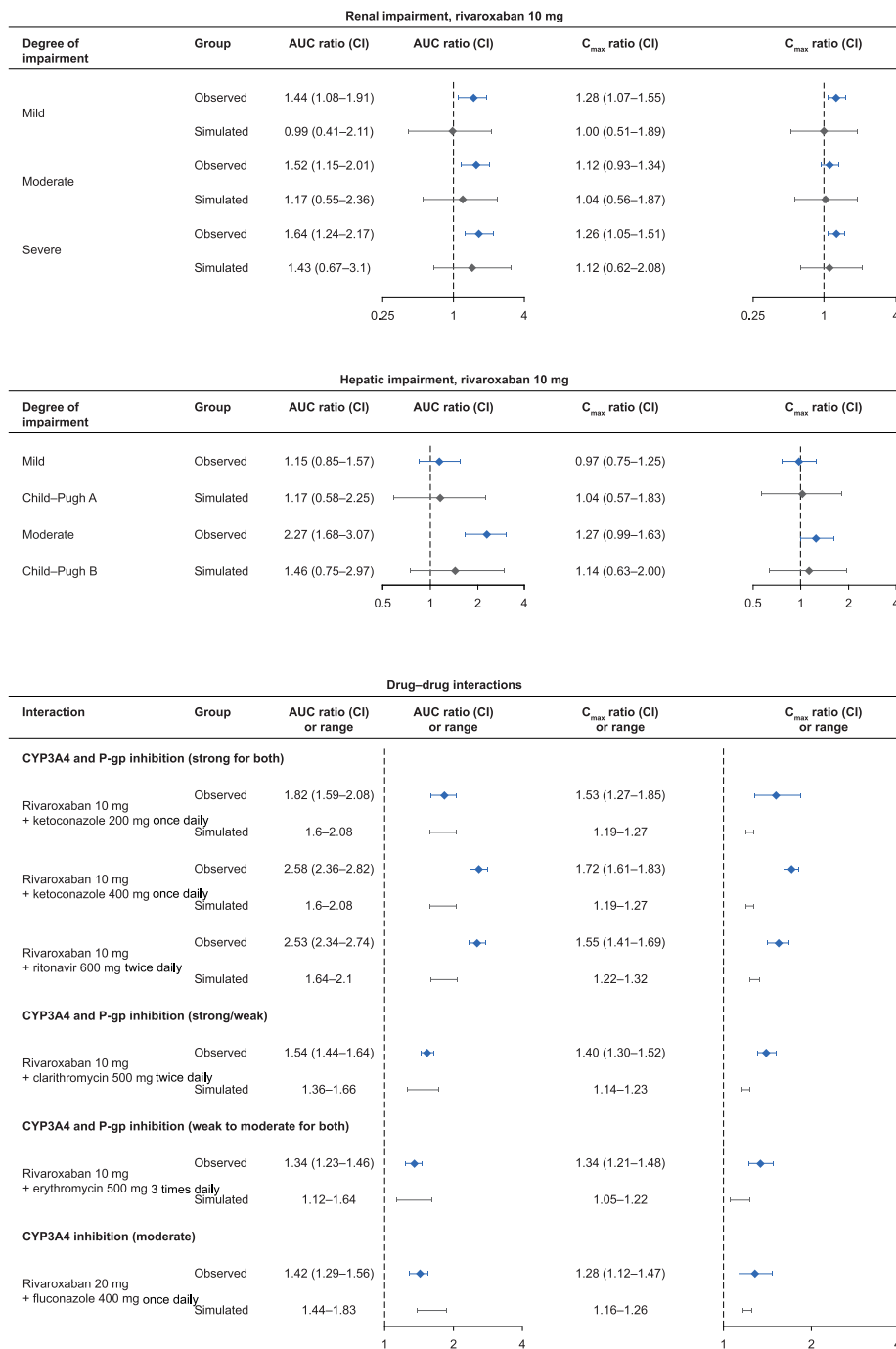


Figure 2. Rivaroxaban exposure derived from clinically observed plasma concentration data and predicted with PBPK simulations in populations with renal impairment, hepatic impairment, or drug–drug interactions.^{11,15,16} AUC and C_{max} are given as mean ratios and 90%CI values for renal and hepatic impairment studies (clinical and simulated) and clinical drug–drug interaction studies. AUC and C_{max} ratios in simulated drug–drug interaction studies are given as ranges associated with the respective ranges of CYP and P-gp inhibition. AUC, area under the concentration–time curve; CI, confidence intervals; C_{max}, maximum plasma concentration; CYP, cytochrome P450; PBPK, physiologically based pharmacokinetic; P-gp, P-glycoprotein.

Renal Impairment

Simulations of rivaroxaban PK following the administration of a single 10-mg dose to populations with renal impairment in the fasted state yielded AUC values and ratios as shown in Figure 2, alongside the data from clinical observations. Mild or moderate renal

impairment was predicted to have almost no impact on rivaroxaban AUC, whereas severe renal impairment was predicted to cause a slight increase in AUC. The observed data showed a higher impact of renal impairment on AUC and C_{max} compared with the simulation in patients with mild, moderate, or severe

Table 4. Predicted Relative Increases in the AUC for Rivaroxaban Resulting From CYP3A4 and P-gp Inhibition

Level of CYP3A4 inhibition ^a	Level of P-gp Inhibition			
	0% to <25%	25% to <50%	50% to <75%	75% to <100%
None	1.00–1.11	1.07–1.20	1.15–1.30	1.24–1.42
Weak (eg, amiodarone) ^b	1.05–1.21	1.12–1.31	1.21–1.43	1.31–1.58
Moderate (eg, dronedarone) ^b	1.13–1.35	1.22–1.48	1.32–1.63	1.44–1.82
Strong	1.26–1.51	1.36–1.66	1.49–1.85	1.64–2.10

AUC, area under the concentration-time curve; CYP, cytochrome P450; FDA, US Food and Drug Administration; P-gp, P-glycoprotein.

^a Based on FDA criteria, using midazolam as the sensitive index substrate.

^b Factors of AUC increase for rivaroxaban in combination with amiodarone or dronedarone as a CYP3A4 inhibitor without an exactly known level of P-gp inhibition.

renal impairment (Figure 2). Associated interindividual variability in AUC and C_{max} , which is represented by the ranges in Figure 2, was predicted to be higher than previously observed.

Hepatic Impairment

Simulations of rivaroxaban PK following the administration of a single 10-mg dose to populations with hepatic impairment in the fasted state yielded AUC values and ratios as shown in Figure 2, alongside the data from clinical observations. As expected, a more severe hepatic impairment resulted in higher AUC for rivaroxaban. With mild hepatic impairment, the predicted AUC and C_{max} were consistent with previously observed values, and the predicted interindividual variability was slightly higher than previously observed (Figure 2). With moderate hepatic impairment, the predicted AUC is on average lower than the observed AUC (–54.1%), but the predicted range overlaps with the observed, and the predicted C_{max} is slightly lower than the observed C_{max} (–11.4%). The predicted interindividual variability was comparable to previous observations.

Drug-Drug Interactions

The concomitant administration of drugs that inhibit the same clearance and elimination pathways can lead to DDIs. The administration of the CYP3A4 and P-gp inhibitors ketoconazole, ritonavir, clarithromycin, erythromycin, and fluconazole with rivaroxaban was assessed with the PBPK model and compared with previous clinical observations in healthy subjects. As expected, the AUC and C_{max} of rivaroxaban increased with the strength of the inhibitors. The simulated increase was also greater with stronger inhibitors in clinical observations, although the simulation underestimated the ranges for C_{max} in most cases (Figure 2). For the lower end of the C_{max} range, the relative deviation between the simulated and observed ranged from –42.0% (rivaroxaban 10 mg + ketoconazole 40 mg once daily) to +4.0% (rivaroxaban 20 mg + fluconazole

400 mg once daily). For the upper end of the C_{max} range, the relative deviation between the simulated and observed ranged from –45.7% (rivaroxaban 10 mg + ketoconazole 200 mg once daily) to –16.7% (rivaroxaban 20 mg + fluconazole 400 mg once daily).

Additional simulations were carried out to assess the possible impact of CYP3A4 and P-gp inhibition, including with the antiarrhythmic agents amiodarone and dronedarone, on the PK of rivaroxaban (Table 4). The model predicted a small to moderate increase in rivaroxaban AUC in combination with dronedarone or amiodarone.

Discussion

PBPK modeling systematically integrates preclinical and clinical knowledge on the PK of a drug as it becomes available during clinical development. A PBPK model consists of drug-dependent and system-dependent parts. The drug-dependent part requires the physicochemical properties of the drug (eg, molecular weight, lipophilicity, and pK_a), which are mostly determined in vitro. The system-dependent part is the mechanistic representation of the physiology and anatomy of the system, such as the organism to which the drug is administered. System compartments in PBPK modeling represent real anatomic spaces, such as intracellular, vascular (plasma and red blood cells), and interstitial spaces or organs. The concentration of a drug in a specific compartment is simulated on the basis of a large set of mass balance equations that describe the absorption, distribution, metabolism, and elimination of a drug in a whole-body PBPK model.²⁷

The modular structure of a PBPK model allows the translation of a model to a different system, such as an untested patient population, by adapting only the system-dependent parameters. For example, scaling of adult PBPK models to children is an established workflow²⁸ that accounts for age-dependent differences in drug clearance and protein binding. Such an approach was used to inform the rivaroxaban dosing

regimen assessed in clinical studies on children.²³ Similarly, the PK of a drug in patient populations with impaired drug clearance can be explored with PBPK modeling by simulating renal or hepatic impairment in the physiologic input parameters.²⁹ The details of PBPK modeling methodology have been described previously.^{30–32} Despite the increasing acknowledgment of PBPK modeling, the large number of required input parameters is a known limitation of this modeling technique. PBPK model input parameters can be physiologic in nature (eg, organ volumes, blood flow rates), compound specific (eg, lipophilicity, solubility), or a mixture of both (eg, organ:plasma partition coefficients that are derived using physicochemical and physiologic information).²⁵ Therefore, the impact of unknown or uncertain parameters and the corresponding inferences made regarding the simulated PK of a drug need to be carefully assessed, for example with a sensitivity analysis.³³ A parameter sensitivity analysis performed with the rivaroxaban PBPK model revealed that the model parameters with the highest sensitivities, with respect to AUC and C_{\max} are physiologic parameters that affect either the absorption or elimination of rivaroxaban. C_{\max} is also affected by the physiologic parameters of the main distribution organs (fat and muscle). A high sensitivity in combination with an uncertain model parameter is associated with a high uncertainty of the model output.

The clinical development of rivaroxaban has been supported by PBPK modeling. This type of modeling is a mathematical tool widely used in pharmaceutical research and development and academia.^{34,35} PBPK modeling was originally established in environmental toxicology and risk assessment.^{36,37} Over the past decades, PBPK modeling has gained importance in making informed decisions during drug development and in the regulatory decision-making process.³⁸ The European Medicines Agency and US Food and Drug Administration have both issued guidelines on the content, conduct, and reporting of PBPK modeling analyses^{39,40} that reflect the ongoing discussion on a scientific framework for PBPK.^{41–44} PBPK modeling has been acknowledged in regulatory guidelines on hepatic impairment,⁴⁵ pediatrics,⁴⁶ and DDI^{46,47} to inform clinical study design. Indeed, the number of regulatory submissions using PBPK modeling has risen constantly over the past years, and a number of drug labels have been informed by PBPK-based simulations (reviewed by Jamei⁴⁸).

In this study, a PBPK model was used to predict the effects of renal impairment, hepatic impairment, and DDIs on the PK of rivaroxaban. The simulated effect of renal or hepatic impairment was generally consistent with previously reported clinical data.^{11,15} However, the simulation predicted a slightly smaller increase in

the AUC and C_{\max} for rivaroxaban compared with clinical data in patients with any renal or moderate hepatic impairment. A previous study also reported smaller predicted increases in rivaroxaban exposure in patients with renal or hepatic impairment compared with observed data.⁴⁹

The concomitant use of rivaroxaban and drugs that are strong inhibitors of both CYP3A4 and P-gp is not recommended because these DDIs could substantially increase the plasma concentration of rivaroxaban and therefore the risk of bleeding. The combination of rivaroxaban with drugs that moderately inhibit CYP3A4 and/or P-gp, or strongly inhibit only one of the elimination pathways, is expected to cause a smaller increase in the plasma concentration of rivaroxaban that can be significant in high-risk patients.^{1–3} The PBPK model predicted increases in the AUC and C_{\max} of rivaroxaban when administered with CYP3A4 or P-gp inhibitors, which increased with the strength of inhibitors. This was consistent with the relationship observed in the clinical data, although the simulated increase in C_{\max} was mostly underestimated (up to –45.7%). The increase in AUC and C_{\max} was larger with strong vs weak inhibitors of CYP3A4 or P-gp in the simulations, as well as in clinical observations.

A potential reason for the tendency to underestimate the effects of comedications on AUC and C_{\max} is the reliability of the fractional clearance contributions of rivaroxaban as implemented in the PBPK model. The main source of information for parameterizing the hepatic and renal contributions is the rivaroxaban mass balance study that reported the radioactive profiles in plasma and excreta of 4 healthy subjects who had received a single oral dose of [¹⁴C]rivaroxaban. The total recovery of radioactivity in humans was 93.7%.⁹ The nonrenal clearance contribution was further subdivided into metabolism by CYP3A4, CYP2J2, and CYP-independent mechanisms based on *in vitro* information.¹⁰ Taken together, the clearance parameterization in the rivaroxaban PBPK model might not 100% accurately reflect the human *in vivo* situation. The parameter sensitivity analysis showed that, in general, parameters that are related to rivaroxaban elimination are among the most sensitive model parameters affecting AUC and C_{\max} predictions. As most sensitive clearance-related parameters, however, the volumes of the liver and kidney and their fractional contributions of cells, vascular, and interstitial space, as well as the kidney blood flow, were identified and not the fractional contributions of hepatic or renal processes to the total rivaroxaban clearance. The American and Canadian labels do not recommend a dose reduction or include a contraindication or warning against the use of the antiarrhythmic agents amiodarone or dronedarone with rivaroxaban in

patients with AF,^{1,3} although the European label and practical guides recommend avoiding the concomitant use of dronedarone and rivaroxaban due to a lack of clinical data.^{2,50} Based on the PBPK model, the predicted increase in AUC with the simultaneous use of rivaroxaban and the weak (amiodarone) and moderate (dronedarone) CYP3A4 and P-gp inhibitors was low and therefore should be unlikely to increase the risk of bleeding in patients receiving rivaroxaban. The findings of our study are also consistent with a subanalysis of the ROCKET AF trial (Rivaroxaban Once Daily Oral Direct Factor Xa Inhibition Compared With Vitamin K Antagonism for Prevention of Stroke and Embolism Trial in Atrial Fibrillation), which demonstrated no increase in the risk of bleeding, mortality, or embolic events in patients with AF receiving concomitant treatment with rivaroxaban and amiodarone or other antiarrhythmic agents.⁵¹

The results of our PBPK modeling analyses are generally consistent with previous studies, including an analysis on DDI between rivaroxaban and amiodarone or dronedarone based on in vitro inhibition assays and static modeling,¹⁸ and a PBPK modeling analysis assessing the effect of DDIs between rivaroxaban and ketoconazole, ritonavir, and clarithromycin.⁴⁹ PBPK modeling and clinical studies have also shown that the potential impact of DDI on rivaroxaban exposure may be of particular concern in patients with renal or hepatic impairment and should be considered in clinical practice.^{49,52–54} The findings of our study provide the data required to address important clinical questions about the optimal management of patients with AF who are receiving rivaroxaban.

Conclusion

Although PBPK models have some limitations, they can be useful for estimating the effects of impaired drug clearance or DDIs on the PK, as in the case of rivaroxaban. Factors in addition to those considered in the PBPK model may also affect the PK of rivaroxaban. If these factors could be identified, the PBPK model could be refined to approximate the real-world PK of rivaroxaban more accurately. Furthermore, the model predictions are consistent with the label recommendations for dose reductions in patients with renal impairment and contraindication in patients with Child-Pugh B and C, and these predictions support the decision not to include a contraindication or warning for the concomitant use of rivaroxaban with dronedarone or amiodarone in patients with AF.

Acknowledgments

The authors thank Lizahn Zwart (Chameleon Communications International), who provided editorial support with funding from Bayer AG and Janssen Scientific Affairs, LLC.

Conflicts of Interest

S.W., K.C., S.K., K.T., M.M., K.F., and W.M. are employees of Bayer AG and may own limited stock of Bayer AG. This manuscript was developed within the scope of their employment and no additional payment was received.

Data Availability Statement

The models developed in this study were based on previously published data.

References

1. Janssen Pharmaceuticals Inc. Xarelto (rivaroxaban) prescribing information. 2020. <http://www.janssenlabels.com/package-insert/product-monograph/prescribing-information/XARELTO-pi.pdf>. Accessed October 5, 2020.
2. Bayer AG. Xarelto[®] (rivaroxaban) summary of product characteristics. https://www.ema.europa.eu/documents/product-information/xarelto-epar-product-information_en.pdf. Published 2020. Accessed July 30, 2020.
3. Bayer Inc. Xarelto[®] (rivaroxaban tablets) product monograph. <http://omr.bayer.ca/omr/online/xarelto-pm-en.pdf>. Published 2019. Accessed February 10, 2020.
4. Monagle P, Lensing AWA, Thelen K, et al. Bodyweight-adjusted rivaroxaban for children with venous thromboembolism (EINSTEIN-Jr): results from three multicentre, single-arm, phase 2 studies. *Lancet Haematol*. 2019;6(10):e500–e509.
5. Male C, Lensing AWA, Palumbo JS, et al. Rivaroxaban compared with standard anticoagulants for the treatment of acute venous thromboembolism in children: a randomised, controlled, phase 3 trial. *Lancet Haematol*. 2020;7(1):e18–e27.
6. Capell WH, Bonaca MP, Nehler MR, et al. Rationale and design for the Vascular Outcomes study of ASA along with rivaroxaban in endovascular or surgical limb revascularization for peripheral artery disease (VOYAGER PAD). *Am Heart J*. 2018;199:83–91.
7. Bonaca MP, Bauersachs RM, Anand SS, et al. Rivaroxaban in peripheral artery disease after revascularization. *N Engl J Med*. 2020;382(21):1994–2004.
8. Plessier A, Denninger MH, Consigny Y, et al. Coagulation disorders in patients with cirrhosis and severe sepsis. *Liver Int*. 2003;23(6):440–448.
9. Weinz C, Schwarz T, Kubitzka D, Mueck W, Lang D. Metabolism and excretion of rivaroxaban, an oral, direct Factor Xa inhibitor, in rats, dogs and humans. *Drug Metab Dispos*. 2009;37(5):1056–1064.
10. Perzborn E, Roehrig S, Straub A, et al. Rivaroxaban: a new oral factor Xa inhibitor. *Arterioscler Thromb Vasc Biol*. 2010;30(3):376–381.
11. Kubitzka D, Becka M, Mueck W, et al. Effects of renal impairment on the pharmacokinetics, pharmacodynamics and safety of rivaroxaban, an oral, direct factor Xa inhibitor. *Br J Clin Pharmacol*. 2010;70(5):703–712.
12. Gnoth MJ, Buetehorn U, Muenster U, Schwarz T, Sandmann S. In vitro and in vivo P-glycoprotein transport characteristics of rivaroxaban. *J Pharmacol Exp Ther*. 2011;338(1):372–380.
13. Wessler JD, Grip LT, Mendell J, Giugliano RP. The P-glycoprotein transport system and cardiovascular drugs. *J Am Coll Cardiol*. 2013;61(25):2495–2502.
14. Mueck W, Stampfuss J, Kubitzka D, Becka M. Clinical pharmacokinetic and pharmacodynamic profile of rivaroxaban. *Clin Pharmacokinet*. 2014;53(1):1–16.

15. Kubitzka D, Roth A, Becka M, et al. Effect of hepatic impairment on the pharmacokinetics and pharmacodynamics of a single dose of rivaroxaban—an oral, direct factor Xa inhibitor. *Br J Clin Pharmacol*. 2013;76(1):89-98.
16. Mueck W, Kubitzka D, Becka M. Co-administration of rivaroxaban with drugs that share its elimination pathways: pharmacokinetic effects in healthy subjects. *Br J Clin Pharmacol*. 2013;76(3):455-466.
17. Grillo JA, Zhao P, Bullock J, et al. Utility of a physiologically-based pharmacokinetic (PBPK) modeling approach to quantitatively predict a complex drug-drug-disease interaction scenario for rivaroxaban during the drug review process: implications for clinical practice. *Biopharm Drug Dispos*. 2012;33(2):99-110.
18. Cheong EJ, Goh JJ, Hong Y, et al. Application of static modeling in the prediction of in vivo drug-drug interactions between rivaroxaban and antiarrhythmic agents based on in vitro inhibition studies. *Drug Metab Dispos*. 2017;45(3):260-268.
19. January CT, Wann LS, Calkins H, et al. 2019 AHA/ACC/HRS focused update of the 2014 AHA/ACC/HRS guideline for the management of patients with atrial fibrillation: a report of the American College of Cardiology/American Heart Association Task Force on Clinical Practice Guidelines and the Heart Rhythm Society in collaboration with the Society of Thoracic Surgeons. *Circulation*. 2019;140(2):e125-e151.
20. Kirchhof P, Benussi S, Kotecha D, et al. 2016 ESC Guidelines for the management of atrial fibrillation developed in collaboration with EACTS. *Eur Heart J*. 2016;37(38):2893-2962.
21. Accord Healthcare Limited. Amiodarone summary of product characteristics. <https://www.medicines.org.uk/emc/product/6018/smpc>. Published 2017. Accessed July 24, 2020.
22. Sanofi-Aventis. Multaq (dronedarone) summary of product characteristics. https://www.ema.europa.eu/en/documents/product-information/multaq-epar-product-information_en.pdf. Published 2020. Accessed June 22, 2020.
23. Willmann S, Becker C, Burghaus R, et al. Development of a paediatric population-based model of the pharmacokinetics of rivaroxaban. *Clin Pharmacokinet*. 2014;53(1):89-102.
24. Stampfuss J, Kubitzka D, Becka M, Mueck W. The effect of food on the absorption and pharmacokinetics of rivaroxaban. *Int J Clin Pharmacol Ther*. 2013;51(7):549-561.
25. Willmann S, Lippert J, Sevestre M, et al. PK-Sim®: a physiologically based pharmacokinetic “whole-body” model. *BIO-SIL-ICO*. 2003;1(4):121-124.
26. US Food and Drug Administration. Drug development and drug interactions: table of substrates, inhibitors and inducers. <https://www.fda.gov/drugs/developmentapprovalprocess/developmentresources/druginteractionslabeling/ucm093664.htm>. Published 2020. Accessed July 24, 2020.
27. Eissing T, Kuepfer L, Becker C, et al. A computational systems biology software platform for multiscale modeling and simulation: integrating whole-body physiology, disease biology, and molecular reaction networks. *Front Physiol*. 2011;2:4.
28. Edginton AN, Schmitt W, Willmann S. Development and evaluation of a generic physiologically based pharmacokinetic model for children. *Clin Pharmacokinet*. 2006;45(10):1013-1034.
29. Edginton AN, Willmann S. Physiology-based simulations of a pathological condition: prediction of pharmacokinetics in patients with liver cirrhosis. *Clin Pharmacokinet*. 2008;47(11):743-752.
30. Upton RN, Foster DJ, Abuhelwa AY. An introduction to physiologically-based pharmacokinetic models. *Paediatr Anaesth*. 2016;26(11):1036-1046.
31. Sager JE, Yu J, Ragueneau-Majlessi I, Isoherranen N. Physiologically based pharmacokinetic (PBPK) modeling and simulation approaches: a systematic review of published models, applications, and model verification. *Drug Metab Dispos*. 2015;43(11):1823-1837.
32. Kuepfer L, Niederalt C, Wendl T, et al. Applied concepts in PBPK modeling: how to build a PBPK/PD model. *CPT Pharmacometrics Syst Pharmacol*. 2016;5(10):516-531.
33. McNally K, Cotton R, Loizou GD. A workflow for global sensitivity analysis of PBPK models. *Front Pharmacol*. 2011;2:31.
34. Luzon E, Blake K, Cole S, et al. Physiologically based pharmacokinetic modeling in regulatory decision-making at the European Medicines Agency. *Clin Pharmacol Ther*. 2017;102(1):98-105.
35. Jones HM, Chen Y, Gibson C, et al. Physiologically based pharmacokinetic modeling in drug discovery and development: a pharmaceutical industry perspective. *Clin Pharmacol Ther*. 2015;97(3):247-262.
36. United States Environmental Protection Agency. *Approaches for the application of physiologically based pharmacokinetic (PBPK) models and supporting data in risk assessment (final report)*. EPA/600/R-05/043F. Washington, DC: US Environmental Protection Agency, Office of Research and Development, National Center for Environmental Assessment. <http://cfpub.epa.gov/ncea/cfm/recordisplay.cfm?deid=157668> Accessed July 24, 2020.
37. World Health Organization. Characterization and application of physiologically based pharmacokinetic models in risk assessment. International Programme on Chemical Safety & Inter-Organization Programme for the Sound Management of Chemicals. Geneva, Switzerland. <http://www.who.int/iris/handle/10665/44495>. Accessed July 24, 2020.
38. EFPIA Mid Workgroup, Marshall SF, Burghaus R, et al. Good practices in model-informed drug discovery and development: practice, application, and documentation. *CPT Pharmacometrics Syst Pharmacol*. 2016;5(3):93-122.
39. European Medicines Agency, Committee for Medicinal Products for Human Use. Guideline on the reporting of physiologically based pharmacokinetic (PBPK) modelling and simulation. <https://www.ema.europa.eu/en/reporting-physiologically-based-pharmacokinetic-pbpbk-modelling-simulation>. Accessed July 24, 2020.
40. US Food and Drug Administration. Physiologically based pharmacokinetic analyses—format and content. <https://www.fda.gov/media/101469/download>. Accessed July 24, 2020.
41. Zhao P, Rowland M, Huang SM. Best practice in the use of physiologically based pharmacokinetic modeling and simulation to address clinical pharmacology regulatory questions. *Clin Pharmacol Ther*. 2012;92(1):17-20.
42. Wagner C, Pan Y, Hsu V, et al. Predicting the effect of cytochrome P450 inhibitors on substrate drugs: analysis of physiologically based pharmacokinetic modeling submissions to the US Food and Drug Administration. *Clin Pharmacokinet*. 2015;54(1):117-127.
43. Wagner C, Pan Y, Hsu V, Sinha V, Zhao P. Predicting the effect of CYP3A inducers on the pharmacokinetics of substrate drugs using physiologically based pharmacokinetic (PBPK) modeling: an analysis of PBPK submissions to the US FDA. *Clin Pharmacokinet*. 2016;55(4):475-483.
44. Sinha V, Zhao P, Huang SM, Zineh I. Physiologically based pharmacokinetic modeling: from regulatory science to regulatory policy. *Clin Pharmacol Ther*. 2014;95(5):478-480.

45. European Medicines Agency. Guideline on the evaluation of the pharmacokinetics of medicinal products in patients with impaired hepatic function. CPMP/EWP/2339/02. http://www.ema.europa.eu/docs/en_GB/document_library/Scientific_guideline/2009/09/WC500003122.pdf. Accessed July 24, 2020.
46. US Food and Drug Administration, Center for Drug Evaluation and Research (CDER). General clinical pharmacology considerations for pediatric studies for drugs and biological products. FDA-2013-D-1275. <https://www.fda.gov/downloads/Drugs/GuidanceComplianceRegulatoryInformation/Guidances/UCM425885.pdf>. Accessed July 24, 2020.
47. European Medicines Agency, Committee for Human Medicinal Products. Guideline on the investigation of drug interactions. CPMP/EWP/560/95/Rev.1 Corr.2. https://www.ema.europa.eu/documents/scientific-guideline/guideline-investigation-drug-interactions_en.pdf. Accessed July 24, 2020.
48. Jamei M. Recent advances in development and application of physiologically-based pharmacokinetic (PBPK) models: a transition from academic curiosity to regulatory acceptance. *Curr Pharmacol Rep*. 2016;2:161-169.
49. Xu R, Ge W, Jiang Q. Application of physiologically based pharmacokinetic modeling to the prediction of drug-drug and drug-disease interactions for rivaroxaban. *Eur J Clin Pharmacol*. 2018;74(6):755-765.
50. Steffel J, Verhamme P, Potpara TS, et al. The 2018 European Heart Rhythm Association practical guide on the use of non-vitamin K antagonist oral anticoagulants in patients with atrial fibrillation. *Eur Heart J*. 2018;39(16):1330-1393.
51. Steinberg BA, Hellkamp AS, Lokhnygina Y, et al. Use and outcomes of antiarrhythmic therapy in patients with atrial fibrillation receiving oral anticoagulation: results from the ROCKET AF trial. *Heart Rhythm*. 2014;11(6):925-932.
52. Moore KT, Vaidyanathan S, Natarajan J, et al. An open-label study to estimate the effect of steady-state erythromycin on the pharmacokinetics, pharmacodynamics, and safety of a single dose of rivaroxaban in subjects with renal impairment and normal renal function. *J Clin Pharmacol*. 2014;54(12):1407-1420.
53. Greenblatt DJ, Patel M, Harmatz JS, et al. Impaired rivaroxaban clearance in mild renal insufficiency with verapamil coadministration: Potential implications for bleeding risk and dose selection. *J Clin Pharmacol*. 2018;58(4):533-540.
54. Ismail M, Lee VH, Chow CR, Rubino CM. Minimal physiologically based pharmacokinetic and drug-drug-disease interaction model of rivaroxaban and verapamil in healthy and renally impaired subjects. *J Clin Pharmacol*. 2018;58(4):541-548.
55. Dzhavad-zade MD, Gasanova EA. [Changes in portal and hepatic blood flow in patients with chronic kidney failure as shown by Doppler ultrasonography]. *Urol Nefrol (Mosk)*. 1998(6):12-15.
56. Meyer-Lehnert H, Bayer T, Predel HG, Glanzer K, Kramer HJ. Effects of atrial natriuretic peptide on systemic and renal hemodynamics and renal excretory function in patients with chronic renal failure. *Klin Wochenschr*. 1991;69(19):895-903.
57. Dowling TC, Briglia AE, Fink JC, et al. Characterization of hepatic cytochrome P4503A activity in patients with end-stage renal disease. *Clin Pharmacol Ther*. 2003;73(5):427-434.
58. Annet L, Materne R, Danse E, et al. Hepatic flow parameters measured with MR imaging and Doppler US: correlations with degree of cirrhosis and portal hypertension. *Radiology*. 2003;229(2):409-414.
59. Dincer D, Besisk F, Demirkol O, et al. Relationships between hemodynamic alterations and Child-Pugh Score in patients with cirrhosis. *Hepatogastroenterology*. 2005;52(65):1521-1525.
60. Chawla Y, Santa N, Dhiman RK, Dilawari JB. Portal hemodynamics by duplex Doppler sonography in different grades of cirrhosis. *Dig Dis Sci*. 1998;43(2):354-357.
61. Froomes PR, Morgan DJ, Smallwood RA, Angus PW. Comparative effects of oxygen supplementation on theophylline and acetaminophen clearance in human cirrhosis. *Gastroenterology*. 1999;116(4):915-920.
62. Woitas RP, Stoffel-Wagner B, Flommersfeld S, et al. Correlation of serum concentrations of cystatin C and creatinine to inulin clearance in liver cirrhosis. *Clin Chem*. 2000;46(5):712-715.
63. Barry M, Keeling PW, Weir D, Feely J. Severity of cirrhosis and the relationship of alpha 1-acid glycoprotein concentration to plasma protein binding of lidocaine. *Clin Pharmacol Ther*. 1990;47(3):366-370.
64. Wong F, Girgrah N, Graba J, et al. The cardiac response to exercise in cirrhosis. *Gut*. 2001;49(2):268-275.
65. Virgolini I, Muller C, Angelberger P, et al. Functional liver imaging with 99Tcm-galactosyl-neoglycoalbumin (NGA) in alcoholic liver cirrhosis and liver fibrosis. *Nucl Med Commun*. 1991;12(6):507-517.
66. George J, Murray M, Byth K, Farrell GC. Differential alterations of cytochrome P450 proteins in livers from patients with severe chronic liver disease. *Hepatology*. 1995;21(1):120-128.
67. Proulx NL, Akbari A, Garg AX, et al. Measured creatinine clearance from timed urine collections substantially overestimates glomerular filtration rate in patients with liver cirrhosis: a systematic review and individual patient meta-analysis. *Nephrol Dial Transplant*. 2005;20(8):1617-1622.
68. Sansoe G, Ferrari A, Castellana CN, et al. Cimetidine administration and tubular creatinine secretion in patients with compensated cirrhosis. *Clin Sci (Lond)*. 2002;102(1):91-98.